

University of Groningen

Work function anisotropy and surface stability of half-metallic CrO(2)

Attema, J. J.; Uijtewaal, M. A.; de Wijs, G. A.; de Groot, R. A.

Published in:
Physical Review. B: Condensed Matter and Materials Physics

DOI:
[10.1103/PhysRevB.77.165109](https://doi.org/10.1103/PhysRevB.77.165109)

IMPORTANT NOTE: You are advised to consult the publisher's version (publisher's PDF) if you wish to cite from it. Please check the document version below.

Document Version
Publisher's PDF, also known as Version of record

Publication date:
2008

[Link to publication in University of Groningen/UMCG research database](#)

Citation for published version (APA):

Attema, J. J., Uijtewaal, M. A., de Wijs, G. A., & de Groot, R. A. (2008). Work function anisotropy and surface stability of half-metallic CrO(2). *Physical Review. B: Condensed Matter and Materials Physics*, 77(16), Article 165109. <https://doi.org/10.1103/PhysRevB.77.165109>

Copyright

Other than for strictly personal use, it is not permitted to download or to forward/distribute the text or part of it without the consent of the author(s) and/or copyright holder(s), unless the work is under an open content license (like Creative Commons).

The publication may also be distributed here under the terms of Article 25fa of the Dutch Copyright Act, indicated by the "Taverne" license. More information can be found on the University of Groningen website: <https://www.rug.nl/library/open-access/self-archiving-pure/taverne-amendment>.

Take-down policy

If you believe that this document breaches copyright please contact us providing details, and we will remove access to the work immediately and investigate your claim.

Downloaded from the University of Groningen/UMCG research database (Pure): <http://www.rug.nl/research/portal>. For technical reasons the number of authors shown on this cover page is limited to 10 maximum.

Work function anisotropy and surface stability of half-metallic CrO₂

J. J. Attema,¹ M. A. Uijttewaai,^{1,*} G. A. de Wijs,¹ and R. A. de Groot^{1,2,†}

¹*ESM, IMM, Radboud University, Toernooiveld 1, 6525ED Nijmegen, The Netherlands*

²*Zernike Institute for Advanced Materials, Nijenborgh 6, 9747AG Groningen, The Netherlands*

(Received 8 October 2007; revised manuscript received 20 February 2008; published 4 April 2008)

Insight in the interplay between work function and stability is important for many areas of physics. In this paper, we calculate the anisotropy in the work function and the surface stability of CrO₂, a prototype half-metal, and find an anisotropy of 3.8 eV. An earlier model for the relation between work function and surface stability is generalized to include the transition-metal oxides. We find that the lowest work function is obtained for surfaces with the most electropositive element, whereas the stable surfaces are those containing the element with the lowest valency. Most CrO₂ surfaces considered remain half-metallic, thus the anisotropy in the work function can be used to realize low resistance, half-metallic interfaces.

DOI: [10.1103/PhysRevB.77.165109](https://doi.org/10.1103/PhysRevB.77.165109)

PACS number(s): 73.30.+y, 75.30.Gw, 72.25.Mk, 73.20.At

I. INTRODUCTION

Electron-emitting materials are applied in many established areas of technology, for example, vacuum electronic devices such as cathode-ray tubes, microwave devices, and free electron lasers. They are also of interest in emerging technologies such as organic light emitting diodes and spintronics, which can benefit from an understanding of the work function.

An important aspect of the electron-emitting properties of the cathode material is the work function. The lifetime of the device is related to the surface stability and the applied voltage. This often implies that cathodes need to have both a low work function and a high surface stability. At first, these requirements appear to be incompatible: A low work function means loosely bound electrons, implying a less stable surface. This reasoning holds for the elements. For instance, cesium has a low work function (2.14 eV) but it is highly reactive, whereas gold is stable but has a high work function (5.1 eV).¹ Experimental results for alloys suggest the alloy effect: The work function and surface stability interpolate between those of the constituting elements.² However, recent theoretical work has shown a different picture for intermetallic compounds. If a compound allows the formation of a surface of nonstoichiometric composition and charge transfer occurs, surfaces with a resulting surface dipole are possible. This surface dipole, depending on its orientation, raises or lowers the work function. The work function may be lowered to even below the work functions of the constituting elements. This was first demonstrated in a computational study for BaAl₄.³ The barium terminated (001) surface has a work function of 1.95 eV, which is lower than that of elemental barium (2.32 eV). It is even lower than that of any element, which is clearly in contradiction with the alloy effect. It is important to notice that the work function for polar compounds, i.e., compounds containing atoms with different electronegativities, is expected to show a large anisotropy, as the surface dipole depends on surface orientation. For BaAl₄ and similar compounds, the surface with the lowest work function was calculated to be the most stable as well. This was explained by the lower electronegativity of barium.^{4,5} The following model was formulated: For an intermetallic

compound with polar surfaces, the difference in electronegativity determines the work function, and the most stable surface has the lowest work function.

Electron injection is also important for spin injection, i.e., spintronics. Spintronics aims to integrate the control of spin degrees of freedom with the conventional charge based electronics. For spin injection, a source of spin polarized electrons is needed. Materials considered for spin injection are half-metals, as they intrinsically have 100% spin polarization. Work on spin injection further focuses on obtaining a spin polarization as high as possible at surfaces and interfaces.^{6,7} Recently, the importance of electrical band engineering for spin injection has become apparent.^{8,9} Ideally, the states carrying the current on either side of the interface are aligned. However, in practice, there is a difference in chemical potential (see Fig. 1). This difference in potential causes a barrier at the interface and reduces the electrical efficiency of the spin injection. Although an interface is more complex than two surfaces, some properties of the two individual surfaces carry over to the interface. In a first approximation, the height of the interface barrier is related to the work function of the two separate surfaces.¹⁰ For a given half-metal/semiconductor interface, the anisotropy in work

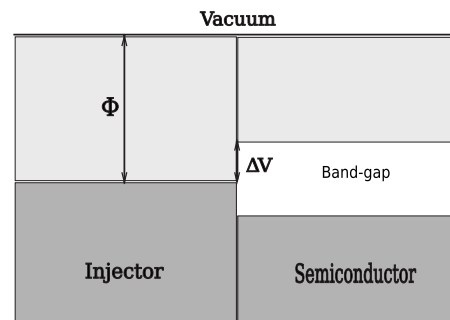


FIG. 1. A schematic drawing of the energy levels of an electron injector/semiconductor interface. Filled and empty states are shaded dark and light gray, respectively. The work function of the injector (Φ) is the difference between the chemical potential in the bulk and the vacuum potential. A mismatch in the chemical potential of the injector and conduction band of the semiconductor results in a potential barrier at the interface (ΔV).

function can be used to minimize the potential barrier.

We will extend the applicability of the model and include materials that are of interest for spintronic applications: transition-metal oxides. In this paper, we investigate the anisotropy in the work function and the surface stability of ferromagnetic CrO_2 . CrO_2 is widely studied; it is a half-metal in calculations and it has experimentally shown a very high spin polarization.¹¹ The main difference between intermetallics and transition-metal oxides is in the combination of electronegativity and valency. For intermetallic compounds, the most electropositive atom also has the lowest valency, resulting in stable, low work function surfaces. For transition-metal oxides, the situation is reversed: The lowest valency occurs almost always for the most electronegative atom, in this case oxygen. Another difference between transition-metal oxides and the previously studied compounds is the occurrence of magnetism. They will provide a challenging test for the model.

This paper is organized as follows. First, we describe the computational method. Then results on bulk CrO_2 are briefly discussed. Results on the structural relaxation are presented, followed by the work functions and surface stabilities, and an outlook.

II. COMPUTATIONAL METHOD

The calculations were carried out using density functional theory with the PW91 generalized gradient approximation functional.^{12,13} We employed projector augmented plane waves^{14,15} as implemented in the Vienna *ab initio* simulation package (VASP).^{16–18} The kinetic energy cutoff was set to 400 eV. The Brillouin zone was sampled with a Monkhorst–Pack mesh with a $6 \times 6 \times 8$ grid for bulk CrO_2 , $1 \times 6 \times 8$ for the (100) surfaces, $1 \times 4 \times 8$ for the (110) surfaces, and $7 \times 7 \times 1$ for the (001) and (011) surfaces. The work functions and surface stabilities were calculated using a supercell approach. The supercell contained slabs with thicknesses of six bulk unit cells for (001), (100), and (011), and eight bulk unit cells for (110), and at least 10 Å of vacuum. We used a minimal unit cell in the directions parallel to the surface. Surface reconstructions involving more than one unit cell or the formation of a Cr_2O_3 surface was not considered. The surfaces at both sides of the slab were taken identical; therefore, some slabs are nonstoichiometric. During relaxation, the central region of the slab was held fixed to obtain faster convergence.

III. BULK CrO_2

Experimentally, CrO_2 is a ferromagnet with a Curie temperature of 386 K.¹⁹ The half-metallic character of CrO_2 and several CrO_2 surfaces (100 and 110) has been shown using spin-resolved photoemission,^{20,21} x-ray absorption,^{22,23} optical spectroscopy,²⁴ and point contact Andreev reflection.²⁵ Earlier photoemission measurements found a small intensity near E_F only, but this was probably due to surface disorder or the formation of Cr_2O_3 at the surface.²⁰

Basically, CrO_2 is an ionic compound containing Cr^{4+} and O^{2-} . It has a magnetic moment of $2\mu_B/\text{f.u.}$, located almost

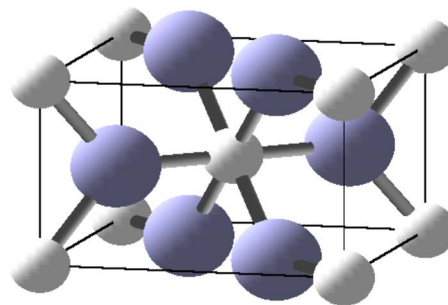


FIG. 2. (Color online) A CrO_2 unit cell. Oxygen atoms are large (blue), while chromium atoms are small (white).

entirely on the chromium atoms. The half-metallic property of CrO_2 is mainly caused by its chemical composition, i.e., the chromium valency, rather than the crystal structure. CrO_2 is a strong magnet, the chromium magnetic moment does not depend on the size of the exchange splitting, as can be seen from the density of states in Fig. 3.

The crystal structure of CrO_2 is depicted in Fig. 2. It crystallizes in the rutile structure, space group $P4_2/mnm$ (No. 136), with experimental lattice parameters $a = 4.4218$ Å and $c = 2.9182$ Å. The chromium is at position $2a$, oxygen is at position $4f$ with parameter $x = 0.301$.²⁶ The chromium atoms are almost perfectly octahedrally surrounded by oxygen atoms, with Cr-O distances of 1.90 and 1.89 Å; each oxygen atom has three chromium neighbors.

The calculated electronic structure of bulk CrO_2 has been extensively studied before.^{27,28} Special attention has been given to the importance of correlation effects.^{29,30} Because we are interested in structural optimizations and work functions, i.e., electrostatics, local density approximation (LDA) is adequate. In view of the comparison between LDA and LDA+ U and the experiment made in Ref. 29, we do not expect that the latter performs better for our purposes. After relaxation of the lattice parameters and the positional parameter of the oxygen atoms, we found $a = 4.405$ Å, $c = 2.905$ Å with the oxygen at position $4f$, and $x = 0.303$. The calculated parameters agree with the experimental values

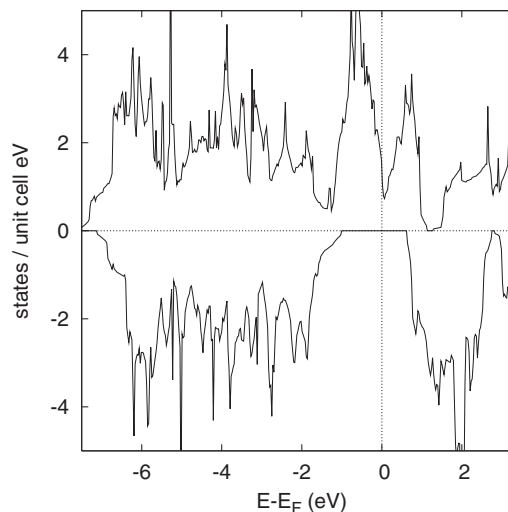


FIG. 3. Calculated density of states for CrO_2 .

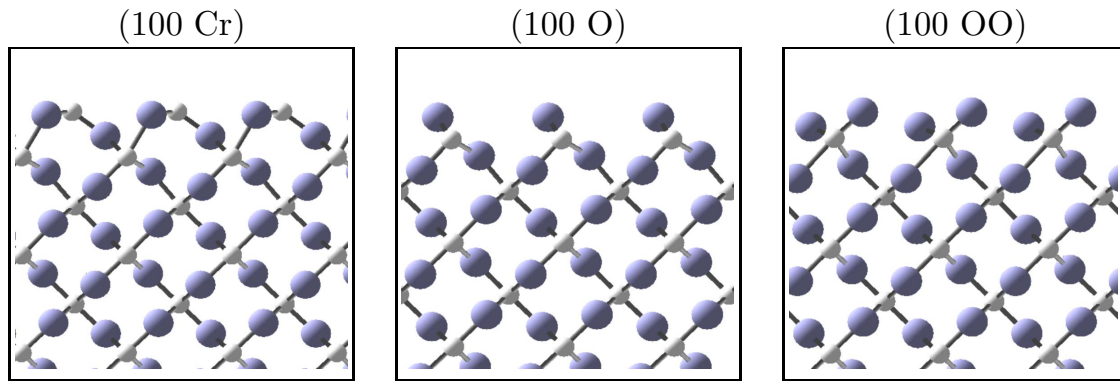


FIG. 4. (Color online) A view along $[001]$ of the relaxed (100) surfaces. The top of the figure is the surface facing the vacuum, while the bottom is toward the bulk. Oxygen atoms are large (blue), while chromium atoms are small (white).

(within 0.5%) and they will be used in this paper. For convenience, we show the calculated density of states in Fig. 3. It shows the crystal field splitting of the chromium $4d$ band. As the chromium atoms have an octahedral coordination, its d band splits into a threefold degenerate t_{2g} band and a doubly degenerate e_g band. The t_{2g} band shows additional structure due to the deviation from perfect octahedral symmetry. In the minority spin direction, the exchange interaction shifts the chromium $4d$ band completely above the Fermi level and opens a band gap.

IV. SURFACES OF CrO_2

Although bulk CrO_2 is a half-metal, it is not *a priori* clear that surfaces of CrO_2 should be half-metallic. For NiMnSb , the first discovered and, consequently, the most extensively studied half-metal, surfaces and interfaces are generally not half-metallic.³¹ The half-metallic character of NiMnSb is a consequence of the specific symmetry in the bulk. This symmetry is destroyed at the interface and, therefore, the half-metallic character is lost; only with careful engineering can half-metallic interfaces be constructed.⁷ However, for CrO_2 , surfaces will be half-metallic as long as the chromium valency is conserved. Indeed, earlier calculations for the (001) surface showed that the half-metallic character was maintained.^{32,33}

In this section, we will first describe in detail the calculated surfaces, both before and after structural relaxation, and we will compare with the literature where available. At the end of the section, general conclusions will be presented.

A. (100) surfaces

Three different (100) surfaces can be constructed: One surface containing a chromium atom (100 Cr), one surface terminating with a single oxygen layer (100 O), and one surface terminating with two oxygen layers (100 OO) (see Fig. 4).

For the (100 Cr) surface, the chromium in the first layer shifts 0.11 \AA inward. It has only three oxygen neighbors and, after relaxation, the nearest neighbor distance is 1.80 \AA on average. The oxygen atoms move -0.28 and 0.15 \AA along $[010]$, and 0.61 and 0.24 \AA outward for the second and fifth

layers. The third layer moves 0.13 \AA outward. The relaxed structure agrees with the calculations reported by Hong and Che³³

Upon relaxation of the (100 O) surface, chromium atoms in the second layer shift -0.10 \AA along $[010]$. The second and fifth layers also shift 0.10 \AA outward. The oxygen atoms shift 0.24 and 0.16 \AA along $[010]$, and 0.20 and 0.28 \AA outward for the first and third layers, respectively. Compared to that of Hong and Che, the relaxation parallel to the surface is similar, but our shift perpendicular to the surface is larger.

For the (100 OO) surface, the first oxygen moves 0.18 \AA outward and the oxygens in the fourth layer move 0.14 \AA outward. The chromium atoms in the third layer move 0.41 \AA outward and 0.15 \AA along $[010]$, while the chromium atoms in the sixth layer move 0.14 \AA outward. The oxygen atom in the top layer has only one chromium neighbor and, as a result, the Cr-O distance after relaxation is reduced to 1.59 \AA .

B. (001) surface

In the $[001]$ direction, only one termination is possible (see Fig. 5). The surface is stoichiometric, containing one Cr and two O atoms. The oxygen atoms in the top layer have

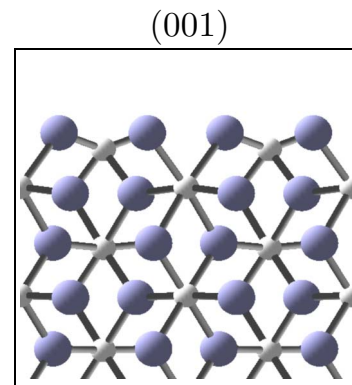


FIG. 5. (Color online) A view along $[100]$ of the relaxed (001) surface. The top of the figure is the surface facing the vacuum, while the bottom is toward the bulk. Oxygen atoms are large (blue), while chromium atoms are small (white).

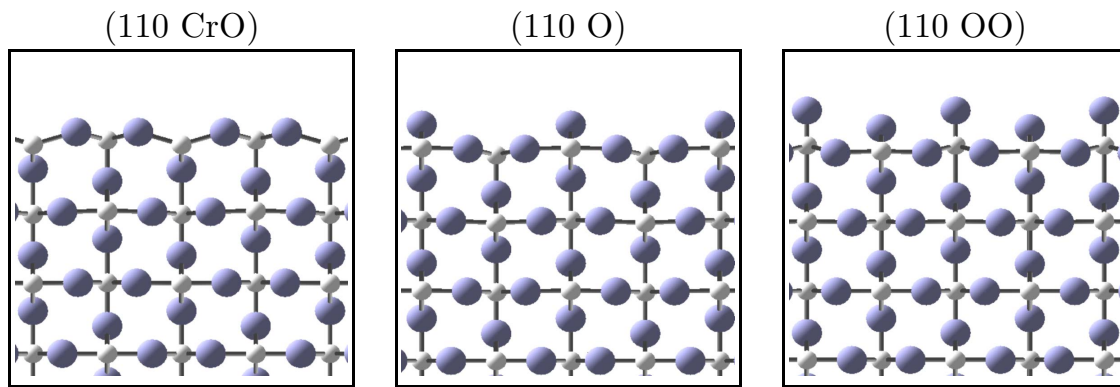


FIG. 6. (Color online) A view along $[001]$ of the relaxed (110) surfaces. The top of the figure is the surface facing the vacuum, while the bottom is toward the bulk. Oxygen atoms are large (blue), while chromium atoms are small (white).

lost one chromium neighbor, while the chromium has four oxygen neighbors. After relaxation, the chromium atoms move 0.15 \AA inward and 0.23 \AA outward for the first and second layers, respectively. The oxygen atoms in the first layer move 0.31 \AA outward and 0.23 \AA along $[110]$ toward the nearest chromium atom. The Cr-O distance for the surface oxygens is 1.72 \AA .

C. (110) surfaces

In the (110) direction, there are again three different terminations. One containing two oxygen and two chromium atoms ((110 CrO)), and two surfaces containing one oxygen [the (110 O) and (110 OO) surfaces] (see Fig. 6).

After relaxation of the (110 CrO) surface, the fivefold surrounded chromium atom in the top layer moves 0.16 \AA outward, while the fourfold surrounded chromium atom moves 0.05 \AA inward. The oxygen atoms in the first layer move 0.51 \AA outward. The second and third oxygen layers move 0.10 \AA and 0.21 \AA outward.

Adding another oxygen layer gives the (110 O) surface. Upon relaxation, the oxygen in the first layer moves 0.10 \AA outward. The oxygens in the second layer move 0.24 \AA outward. The second layer also contains two chromium atoms, one with five oxygen neighbors and one with six neighbors. The sixfold surrounded chromium moves 0.27 \AA outward, while the fivefold surrounded chromium moves slightly in-

ward. The third layer oxygen moves 0.13 \AA outward.

Finally, the (110 OO) surface is obtained by adding another oxygen layer. All chromium atoms have a bulklike sixfold coordination, but the first two oxygen layers have missing neighbors. The first layer oxygen atom has only one neighboring chromium, while the second layer oxygen atoms has two. The oxygens in the first layer relax 0.11 \AA outward. In the third layer, one chromium moves 0.41 \AA outward, reducing the distance with the first layer oxygen to 1.59 \AA ; the other chromium moves 0.15 \AA outward.

D. (011) surfaces

In the (011) direction (see Fig. 7), CrO_2 consists of planes containing either two oxygen or two chromium atoms. There are three possible terminations: a chromium terminated surface ((011 Cr)), one with a single oxygen layer ((011 O)), and one with a double oxygen layer ((011 OO)).

For the (011 O) , the relaxation has only a small effect. The chromium atoms in the second layer only have five nearest oxygen atoms; they relax slightly outward and move 0.16 \AA along $[100]$. The oxygens in the first layer are also missing a neighbor; they move a little inward and -0.08 \AA along $[100]$. The final Cr-O distance at the surface is 1.81 \AA .

In the (011 OO) surface, the first layer oxygens have only one chromium neighbor. They move 0.23 \AA along $[011]$ and 0.07 \AA inward, reducing the Cr-O distance to 1.59 \AA . The

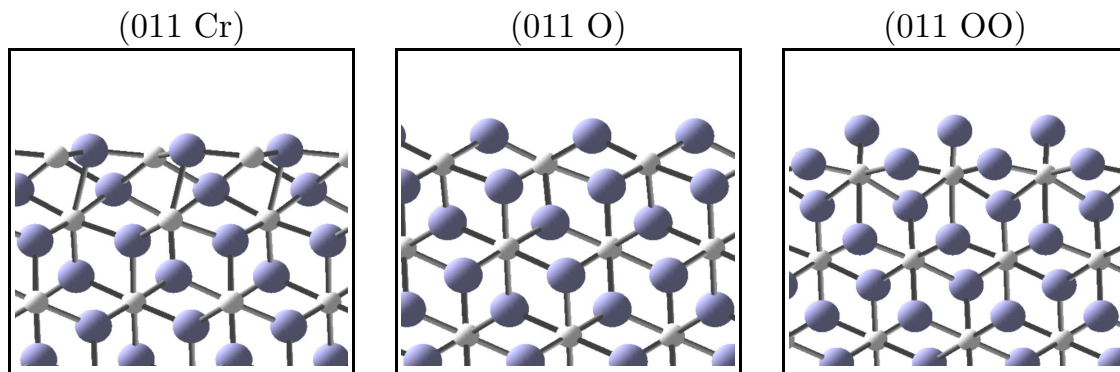


FIG. 7. (Color online) A view along $[100]$ of the relaxed (011) surfaces. The top of the figure is the surface facing the vacuum, while the bottom is toward the bulk. Oxygen atoms are large (blue), while chromium atoms are small (white).

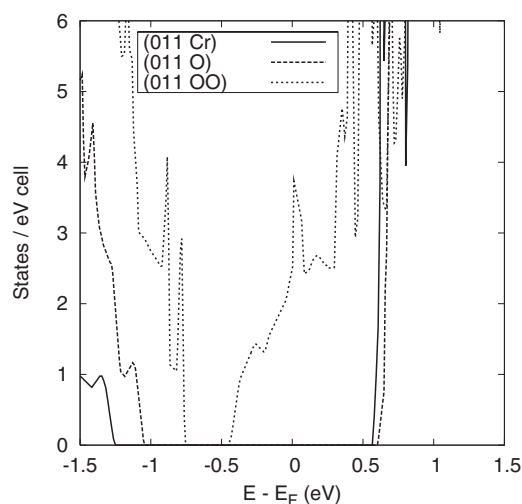


FIG. 8. The density of states for the minority spin direction of the relaxed (011 Cr), (011 O), and (011 OO) slabs.

oxygen atoms in the second layer have two neighbors and they move ± 0.09 Å along [100], 0.18 Å along [011], and 0.14 Å inward. The third layer chromium moves 0.27 Å outward, reducing the Cr-O distance to 1.79 and 1.77 Å.

The chromium terminated surface (011 Cr) shows the largest relaxation. The surface chromiums have only three oxygen neighbors. They relax -1.52 Å along $[01\bar{1}]$ and 0.56 Å inward. The second layer oxygens move -2.15 Å along [011] and 0.31 Å outward, and -0.66 and 0.70 Å along [100]. The first and second layers have merged, forming a mixed chromium / oxide layer. The chromium atoms

are now located above the center of a rectangle formed by two oxygens from the newly formed outer layer and two oxygens from a lower layer.

E. Electronic and magnetic structures

Except for two surfaces, all the surfaces considered here are half-metallic. The unrelaxed (100 OO) surface and the relaxed (011 OO) surface show states in the minority spin band gap, derived from both the chromium and the oxygen atoms. For these slabs, the composition at the surface is too far from stoichiometry and the half-metallicity is lost. The band gap at the surface is largest for chromium terminated surfaces, the (100 Cr), (110 CrO), and (011 Cr). Adding oxygen to the surface decreases the band gap by both lowering the conduction band and raising the valence band (see Fig. 8).

For the stoichiometric slabs, all chromium atoms have approximately the same moment as in bulk CrO_2 . However, for the stoichiometric (001) surface, the moment on the surface chromiums is reduced to $1.3\mu_B$. For nonstoichiometric slabs, the magnetic moment near the surface is determined by the chromium to oxygen ratio. For the chromium rich surfaces, the (100 Cr), (110 CrO), and (011 Cr) surfaces, the magnetic moments of the outermost chromium atoms are 2.9, 2.6, and $3.0\mu_B$, respectively. For the oxygen rich surfaces, the magnetic moment is $0.7\mu_B$ for the (100 OO) and $1.1\mu_B$ for the (110 OO) surface. The (011 OO) surface is no longer half-metallic, and the magnetic moment on the outermost chromium layer ($0.1\mu_B$) has almost disappeared.

TABLE I. Atomic relaxation of the top two layers perpendicular to the surface and the shortest chromium-oxygen distance at the surface. Distances are in Angstrom; positive values are toward the vacuum.

Surface	Top layer	Second layer	Shortest Cr-O
(100 Cr)	Cr -0.11	O 0.61	1.77
(100 O)	O 0.20	Cr 0.10	1.77
(100 OO)	O 0.18	O 0.02	1.59
(001)	Cr -0.15		1.72
	O 0.31		
	O 0.31		
(110 CrO)	Cr 0.16	O 0.10	1.81
	Cr -0.05		
	O 0.51		
	O 0.51		
(110 O)	O 0.10	Cr 0.27	1.78
		Cr -0.04	
		O 0.24	
		O 0.24	
(110 OO)	O 0.11	O -0.03	1.79
(011 Cr)	Cr -0.56	O 0.31	1.83
(011 O)	O -0.02	Cr 0.02	1.80
(011 OO)	O -0.07	O -0.14	1.59

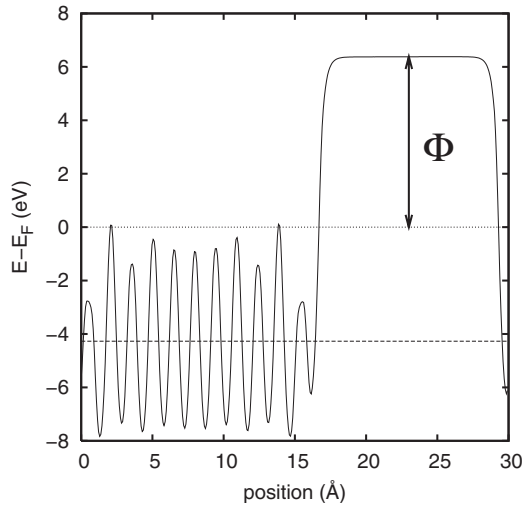


FIG. 9. The electrostatic potential V averaged over a *surface* unit cell of the (001) slab, as a function of the position in the slab. The slab runs from 0 to 16 Å. The dashed line indicates the electrostatic potential averaged over a *bulk* unit cell in the slab center. The position of the Fermi level with respect to the averaged electrostatic potential is taken from a calculation of bulk CrO_2 . The work function Φ is also indicated.

F. Conclusions

The relaxations described in the previous sections have been summarized in Table I, and we can draw the following conclusions. CrO_2 has a tendency to maintain the sixfold coordination of chromium at the surface. Consequently, the chromium moves down into the surface and the oxygen moves upward for chromium or mixed terminated surfaces. To compensate for the lower coordination at the surface, the chromium-oxygen nearest neighbor distances at the surface are reduced by about 5% to 1.82 Å. From this, we can expect a smaller surface dipole for the relaxed surface. For the double oxygen terminated surfaces, some of the oxygens only have a single chromium neighbor compared to three neighbors in the bulk. Upon relaxation, this chromium moves a distance of 1.59 Å from the oxygen, lowering the surface dipole even further.

TABLE II. Work functions for CrO_2 surfaces.

	$\Phi_{\text{unrelaxed}}$ (eV)	Φ_{relaxed} (eV)
(100) Cr	3.64	3.40
(100) O	6.38	6.23
(100) OO	8.59	7.20
(001)	4.72	6.30
(110) CrO	3.16	4.28
(110) O	6.25	5.80
(110) OO	8.45	7.13
(011) Cr	3.38	3.99
(011) O	5.83	5.54
(011) OO	8.06	6.94

V. WORK FUNCTION

The work function is defined as the difference between the Fermi level and the potential in the vacuum far from the surface. These potentials are calculated as described by Fall *et al.*³⁴ For the calculation of an accurate Fermi level, a relatively thick slab is required. However, the average electrostatic potential in the center of the slab converges for much thinner slabs. By combining a highly accurate calculation on bulk CrO_2 for the position of the Fermi level with a converged electrostatic potential of a thin slab, accuracies of a few hundredths of eV for the work function can be achieved. Figure 9 illustrates the procedure for the (001) surface.

The calculated work functions are presented in Table II. The variation in work function is very large (3.8 eV for the relaxed surfaces). This is mainly due to a different surface termination. We see that an increasing oxygen coverage leads to a significant increase in work function from 3.4 eV for the (100 Cr) surface to 7.2 eV for the (100 OO) surface. The work function for the (100 Cr) surface is significantly below the chromium work function (4.5 eV).¹ If we consider only the single oxygen terminated surfaces, the anisotropy is 0.69 eV. For the surfaces with a double oxygen layer, the anisotropy is only 0.26 eV. The lowest work functions and largest anisotropy are found in the mixed oxygen/chromium surfaces and the pure chromium surfaces. For the oxygen terminated surfaces, the relaxation lowers the work function. According to the Smoluchowski³⁵ model, an open surface has a low work function. We expect relaxation to smooth the surface, and this would imply an increase in the work function. However, the decrease in work function can be explained by a smaller dipole moment due to the smaller Cr-O distance at the surface. The smaller dipole at the surfaces also explains the increase in work function for the chromium terminated surfaces. We conclude that the work function is mainly determined by the electronegativity of the surface atoms, with lower electronegativity leading to lower work functions.

VI. SURFACE STABILITY AND ENERGY

Stability is a complex concept: A solid can become unstable in various ways. Some examples are transition toward another crystal structure, roughening or reconstruction of a surface, decomposition of a compound into its constituent elements, and chemical reaction with the atmosphere. The binding energy of a compound defines its stability toward decomposition. The anisotropy in the surface energy determines the stability toward deformation. The stability toward roughening also contains contributions from surfaces of other indices. In fact, each type of stability of a structure originates from an energy difference with a corresponding (transition) state. Thus, lowering the energy of the surface under consideration increases its stability indiscriminately. The (relative) surface energy (γ) will, therefore, be taken as the measure of its stability. In general, crystal surfaces with low energies are formed with large surface areas, and vice versa.³⁶ However, of the different surface terminations with the same index, only the most stable one will be formed.

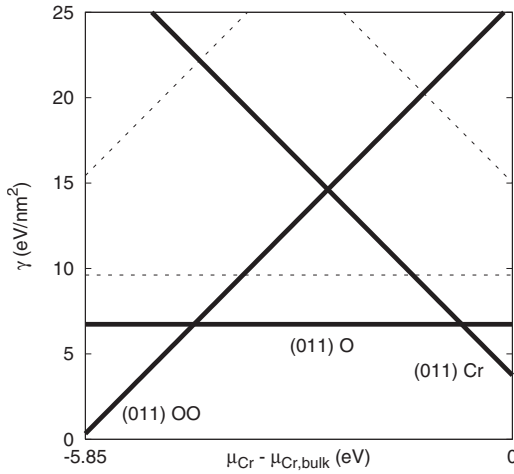


FIG. 10. Surface energy (eV/nm^2) of the different (011) surfaces as function of the chromium chemical potential (μ_{Cr} , eV). Bulk-terminated (dotted lines) and relaxed surfaces (solid lines) are shown. The chemical potential ranges from the chromium bulk one to that minus the binding energy of CrO_2 . The (011) surface with half an oxygen atom per unit cell is stable in the largest part of the plot.

The surface energy is calculated as the difference between the energy of a slab and the equivalent bulk, normalized to unit area. For nonstoichiometric slabs, no equivalent bulk exists. A surface energy can be calculated, nevertheless, that varies with chemical potential, when a thermodynamic equilibrium is assumed between the bulk and reservoirs of the constituting elements.³⁷ For CrO_2 , the chemical potentials of chromium (μ_{Cr}) and oxygen (μ_{O}) are linked to the total energy per formula unit (E_{CrO_2}) of the compound itself:

$$E_{\text{CrO}_2} = \mu_{\text{Cr}} + 2\mu_{\text{O}}. \quad (1)$$

The energy of a general surface is the total energy of a slab with these surfaces exclusively (E_{slab}) minus the number of chromium atoms (N_{Cr}) and oxygen atoms (N_{O}) times their respective chemical potentials and normalized to surface area ($2A_{\text{S}}$). With Eq. (1), μ_{O} can be eliminated in favor of E_{CrO_2} . The energy of surface of nonstoichiometric slabs ($N_{\text{O}} \neq 2N_{\text{Cr}}$) will depend on μ_{Cr} with a slope that is determined by the (relative) difference of the number of oxygen and chromium atoms:

$$2A_{\text{S}}\gamma^{\text{surf}}(\mu_{\text{Cr}}) = E_{\text{slab}} - N_{\text{Cr}}\mu_{\text{Cr}} - N_{\text{O}}\mu_{\text{O}} = E_{\text{slab}} - \frac{N_{\text{O}}}{2}E_{\text{CrO}_2} + \left(\frac{N_{\text{O}}}{2} - N_{\text{Cr}}\right)\mu_{\text{Cr}}. \quad (2)$$

The chromium chemical potential can, in principle, be varied during crystallization. Droplets of chromium or oxygen will form, however, when the chemical potential of the respective element is larger than its elemental bulk energy. This sets reasonable limits on the chemical potentials:

$$\mu_{\text{Cr}} < \mu_{\text{Cr,bulk}}, \quad \mu_{\text{O}} < \mu_{\text{O,molecule}}. \quad (3)$$

When we combine this with the definition of the binding energy as follows:

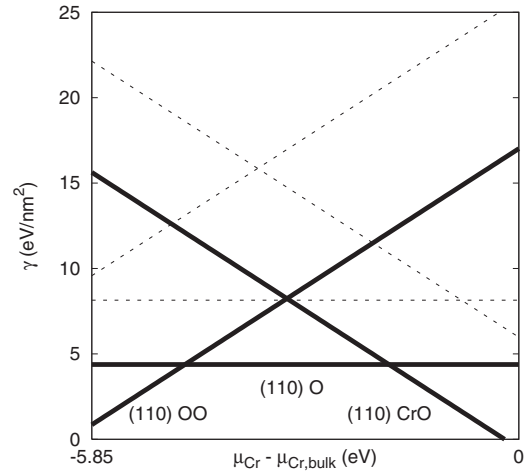


FIG. 11. Surface energy (eV/nm^2) of the different (110) surfaces as function of the chromium chemical potential (μ_{Cr} , eV). Bulk-terminated (dotted lines) and relaxed surfaces (solid lines) are shown. The chemical potential ranges from the chromium bulk one to that minus the binding energy of CrO_2 . The single oxygen (110) surface is stable in the largest part of the plot.

$$E_{\text{CrO}_2,\text{bind}} = E_{\text{Cr,bulk}} + 2E_{\text{O,molecule}} - E_{\text{CrO}_2}, \quad (4)$$

where $E_{\text{Cr,bulk}}$ is the energy of a chromium atom in elemental chromium and $E_{\text{O,molecule}}$ is half the energy of an O_2 molecule, we find the following range of interest for the chromium chemical potential:

$$E_{\text{CrO}_2,\text{bind}} < \mu_{\text{Cr}} - \mu_{\text{Cr,bulk}} < 0. \quad (5)$$

VII. SURFACE STABILITY: RESULTS

We start with the three (011) surfaces. Their surface energies are shown in Fig. 10. The surface energy of the single oxygen surface is relatively low initially and relaxation decreases it by a few eV. This corresponds well to the movement of the atoms at this surface. Both the chromium and the double oxygen surfaces are very unstable initially and are significantly stabilized by relaxation. This can be attributed to the incomplete coordination before and the improved coordination after relaxation of the chromium and oxygen atoms at the surface. In fact, the chromiums at the surface move into the surface past the subsurface oxygens, leading to an oxygen terminated surface. For all three surfaces, a region of stability exists. For the chromium terminated surface, the region is very small, though. The instability of the Cr surface is explained by noting that chromium has six neighbors in the bulk compared to only three neighbors for the oxygen atoms.

The surface energies for the (110) surfaces are shown in Fig. 11. Before relaxation, all three terminations are very unstable. The relaxation considerably changes this picture. Again, stability regions for all three terminations exist, but that of the single O surface is largest.

The surface energies for the (100) surfaces (depicted in Fig. 12) show quite a different situation. The amount of relaxation is moderate for both the Cr and the (single) O ter-

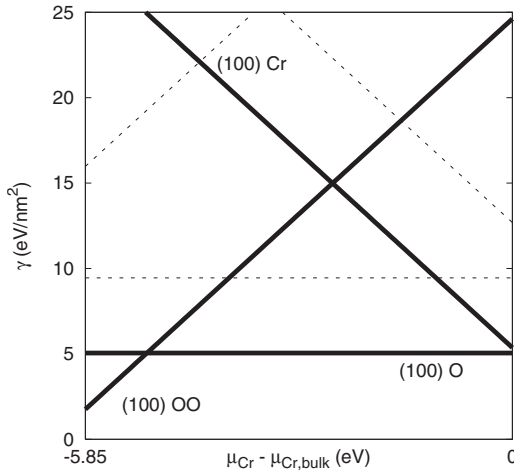


FIG. 12. Surface energy (eV/nm^2) of the different (100) surfaces as function of the chromium chemical potential (μ_{Cr} , eV). Bulk-terminated (dotted lines) and relaxed surfaces (solid lines) are shown. The chemical potential ranges from the chromium bulk one to that minus the binding energy of CrO_2 . The single oxygen surface is the most stable one.

mination and is directed (again) to improve the oxygen coordination of chromium. The outer oxygen at the double oxygen surface has only one Cr neighbor, which explains its initial instability. Here, the largest difference with the other directions is that only oxygen terminated surfaces are stable.

The (001) surface is stoichiometric. The surface is moderately stable initially with a surface energy of $\gamma = 13.76 \text{ eV}/\text{nm}^2$. The relaxation turns the surface into a purely oxygen one, but it stays relatively unstable ($\gamma = 8.34 \text{ eV}/\text{nm}^2$). The cause is the partial coordination of the surface chromium by oxygen, as well. All stable terminations are, in fact, oxygen surfaces even those that are (partially) Cr terminated initially. Moreover, the energy variation is, surprisingly, small. It seems that all the surfaces try to attain a similar surface structure.

Summarizing, we find that for a wide range of the chromium chemical potential, the oxygen terminated surfaces of CrO_2 are the most stable, because those provide an optimal coordination for the chromium atoms. With the same reasoning, the single oxygen terminated surfaces are more stable than the double oxygen terminated surfaces. The double oxygen terminated surfaces contain oxygens with a very low coordination, whereas at the single oxygen terminated surfaces, the oxygen coordination is more like in the bulk. We conclude that the surface stability is predominantly determined by the valency of the surface atoms. For a given index, the most stable surface is generally the one containing atoms with the lowest valency.

VIII. SUMMARY AND DISCUSSION

The surface stability and work function of several CrO_2 surfaces were investigated. We found a large variation (3.8 eV) in the work function. For the relaxed surfaces, the lowest work function is for the chromium terminated (100) surface (3.40 eV) and the highest for the double oxygen ter-

minated (100) surface (7.20 eV). The oxygen terminated surfaces were found to be the most stable ones. All surfaces, except the unrelaxed (100 OO) and the relaxed (011 OO), retained the half-metallic properties.

In previous studies, a model was formulated for the relation between surface stability and work function of a range of intermetallic compounds. For these compounds, the work function showed a large anisotropy. The most stable surfaces also had the lowest work functions.³⁻⁵ In the case of BaAl_4 , this model correctly predicts a Ba terminated surface that also has the lowest work function; the more electropositive element, i.e., Ba, prefers to reside at the surface and, hence, also induces a dipole moment that tends to lower the work function. The other intermetallics studied, CaAl_4 , LaB_6 , Ca_2N , and BaAuIn_3 , exhibited similar behavior. This model fails, however, to explain the instability of the chromium terminated surfaces in CrO_2 . Here, the most stable surface is oxygen terminated, hence the surface dipole moment is unfavorable and increases the work function. Nevertheless, the occurrence of oxygen in the outer layer can be rationalized, as it has a lower valency than Cr. Thus, the Cr prefer to remain immersed below the surface to retain a high coordination. Based on these considerations we can now extend the model: The surface stability is determined by the valency of the atoms, and the atoms with the lowest valency form the most stable surface. The work function is determined by the electronegativity of the atoms, and the surface with the most electropositive atom has the lowest work function. This applies both to intermetallic alloys and compounds combining metallic elements with nonmetallic elements of high valency.

Finally, we would like to discuss the implications of our findings, in particular, for spintronics. Although a conductor/semiconductor interface is different from a surface, the work function of the conductor still gives a reasonable indication of the Schottky barrier of the interface. The large anisotropy found in the CrO_2 work function therefore, suggests a similar anisotropy in the Schottky barrier. By tuning the conditions of the surface preparation, one can choose, in principle, the most favorable surface, e.g., to minimize the barrier height. Experimentally, Min *et al.*⁹ have shown that adding an electropositive element, in their case gadolinium, to a ferromagnet/insulator/semiconductor contact lowers the interface resistance, while the spin tunnel polarization is hardly affected. Alternatively, by preparing different surface terminations of the half-metal CrO_2 , one may attain a similar effect. Of course, the interface dipole is not formed by the metal contact exclusively. Contributions from the semiconductor, interface states, and possibly an insulating barrier material may also play a role.

ACKNOWLEDGMENTS

This work is part of the research program of the Stichting voor Fundamenteel Onderzoek der Materie (FOM); Financial support from the Nederlandse Organisatie voor Wetenschappelijk Onderzoek (NWO), in addition to that from the Technology Foundation (STW) and NanoNed, is gratefully acknowledged. We also wish to thank R. Jansen (UT) for useful discussions.

*Present address: Max-Planck Institut für Eisenforschung, Max-Planck-Straße 1, 40237 Düsseldorf, Germany.

†r.degroot@science.ru.nl

- ¹ *CRC Handbook of Chemistry and Physics* (Chemical Rubber Company, Boca Raton, FL, 1997).
- ² A. H. Nethercot, Jr., *Phys. Rev. Lett.* **33**, 1088 (1974).
- ³ M. A. Uijtewaal, G. A. de Wijs, R. A. de Groot, R. Coehoorn, V. van Elsbergen, and C. H. L. Weijtens, *Chem. Mater.* **17**, 3879 (2005).
- ⁴ M. A. Uijtewaal, G. A. de Wijs, and R. A. de Groot, *Surf. Sci.* **600**, 2495 (2006).
- ⁵ M. A. Uijtewaal, G. A. de Wijs, and R. A. de Groot, *J. Phys. Chem. B* **110**, 18459 (2006).
- ⁶ R. Fiederling, M. Keim, G. Reuscher, W. Ossau, G. Schmidt, A. Waag, and L. W. Molenkamp, *Nature (London)* **420**, 787 (1999).
- ⁷ J. J. Attema, G. A. de Wijs, and R. A. de Groot, *J. Phys. D* **39**, 793 (2006).
- ⁸ W. van Roy, P. van Dorpe, J. de Boeck, and G. Borghs, *Mater. Sci. Eng., B* **128**, 155 (2006).
- ⁹ B.-C. Min, K. Motohashi, C. Lodder, and R. Jansen, *Nat. Mater.* **5**, 817 (2006).
- ¹⁰ J. Bardeen, *Phys. Rev.* **71**, 717 (1947).
- ¹¹ R. Keizer, S. T. B. Goennenwein, T. M. Klapwijk, G. Miao, G. Xiao, and A. Gupta, *Nature (London)* **439**, 825 (2006).
- ¹² J. P. Perdew, J. A. Chevary, S. H. Vosko, K. A. Jackson, M. R. Pederson, D. J. Singh, and C. Fiolhais, *Phys. Rev. B* **46**, 6671 (1992).
- ¹³ S. H. Vosko, L. Wilk, and M. Nusair, *Can. J. Phys.* **58**, 1200 (1980).
- ¹⁴ G. Kresse and D. Joubert, *Phys. Rev. B* **59**, 1758 (1999).
- ¹⁵ P. E. Blöchl, *Phys. Rev. B* **50**, 17953 (1994).
- ¹⁶ G. Kresse and J. Furthmüller, *Phys. Rev. B* **54**, 11169 (1996).
- ¹⁷ G. Kresse and J. Furthmüller, *Comput. Mater. Sci.* **6**, 15 (1996).
- ¹⁸ G. Kresse and J. Hafner, *Phys. Rev. B* **47**, 558 (1993).
- ¹⁹ J. S. Kouvel and D. S. Rodbell, *J. Appl. Phys.* **38**, 979 (1967).
- ²⁰ K. P. Kämper, W. Schmitt, G. Güntherodt, R. J. Gambino, and R. Ruf, *Phys. Rev. Lett.* **59**, 2788 (1987).
- ²¹ Y. S. Dedkov, M. Fonine, C. König, R. U., G. Güntherodt, S. Senz, and D. Hesse, *Appl. Phys. Lett.* **80**, 4181 (2002).
- ²² D. J. Huang, *et al.*, *Phys. Rev. B* **67**, 214419 (2003).
- ²³ Y. S. Dedkov, A. S. Vinogradov, M. Fonin, C. König, D. V. Vyalikh, A. B. Preobrajenski, S. A. Krasnikov, E. Y. Kleimenov, M. A. Nesterov, U. Rudiger, S. L. Molodtsov, G. Guntherodt, *Phys. Rev. B* **72**, 060401(R) (2005).
- ²⁴ H. Huang, K. Seu, A. Reilly, Y. Kadmon, and J. W. F. Egelhoff, *J. Appl. Phys.* **97**, 10C309 (2005).
- ²⁵ G. T. Woods, R. J. Soulen, I. I. Mazin, B. Nadgorny, M. S. Osofsky, J. Sanders, H. Srikanth, W. F. Egelhoff, and R. Datla, *Phys. Rev. B* **70**, 054416 (2004).
- ²⁶ W. H. Cloud, D. S. Schreiber, and K. R. Babcock, *J. Appl. Phys.* **33**, 1193 (1962).
- ²⁷ K. Schwarz, *J. Phys. F: Met. Phys.* **16**, L211 (1986).
- ²⁸ S. Matar, G. Demazeau, J. Sticht, V. Eyert, and J. Kübler, *J. Phys. I* **2**, 315 (1992).
- ²⁹ A. Toropova, G. Kotliar, S. Y. Savrasov, and V. S. Oudovenko, *Phys. Rev. B* **71**, 172403 (2005).
- ³⁰ L. Chioncel, H. Allmaier, E. Arrigoni, A. Yamasaki, M. Daghofer, M. I. Katsnelson, and A. I. Lichtenstein, *Phys. Rev. B* **75**, 140406(R) (2007).
- ³¹ G. A. de Wijs and R. A. de Groot, *Phys. Rev. B* **64**, 020402(R) (2001).
- ³² H. van Leuken and R. A. de Groot, *Phys. Rev. B* **51**, 7176 (1995).
- ³³ F. Hong and J. G. Che, *Appl. Phys. Lett.* **88**, 121903 (2006).
- ³⁴ C. J. Fall, N. Binggeli, and A. Baldereschi, *J. Phys.: Condens. Matter* **11**, 2689 (1999).
- ³⁵ R. Smoluchowski, *Phys. Rev.* **60**, 661 (1941).
- ³⁶ G. Wulff, *Z. Kristallogr.* **34**, 449 (1901).
- ³⁷ J. E. Northrup, *Phys. Rev. B* **44**, 1419 (1991).